Serb. Astron. J. № 198 (2019), 13 - 23
DOI: https://doi.org/10.2298/SAJ190131003V

UDC 520.822 + 524.7 NGC2366 + 524.354
Original scientific paper

OPTICAL OBSERVATIONS OF THE NEARBY GALAXY NGC 2366 THROUGH NARROWBAND Hα AND [SII] FILTERS. SUPERNOVA REMNANTS STATUS*

M. M. Vučetić[1], D. Onić[1], N. Petrov[2], A. Ćiprijanović[1] and M. Z. Pavlović[1]

[1] *Department of Astronomy, Faculty of Mathematics, University of Belgrade, Studentski trg 16, 11000 Belgrade, Serbia*

E–mail: *mandjelic@math.rs, donic@math.rs, aleksandra@math.rs, marko@math.rs*

[2] *Institute of Astronomy and National Astronomical Observatory, Bulgarian Academy of Sciences, 72 Tsarigradsko Shosse Blvd, BG-1784 Sofia, Bulgaria*

E–mail: *nip.sob@gmail.com*

(Received: January 31, 2019; Accepted: February 22, 2019)

SUMMARY: We present detection of 64 H II regions, three superbubbles and two optical supernova remnant (SNR) candidates in the nearby irregular galaxy NGC 2366. The SNR candidates were detected by applying [S II]/Hα ratio criterion to observations made with the 2-m RCC telescope at Rozhen National Astronomical Observatory in Bulgaria. In this paper we report coordinates, diameters, Hα and [S II] fluxes for detected objects across the two fields of view in the NGC 2366 galaxy. Using archival XMM-Newton observations we suggest possible X-ray counterparts of two optical SNR candidates. Also, we discard classification of two previous radio SNR candidates in this galaxy since they appear to be background galaxies.

Key words. ISM: supernova remnants – H II regions – Galaxies: individual: NGC 2366

1. INTRODUCTION

Being explosive events that release large amount of energy ($\sim 10^{51}$ergs) into the interstellar medium (ISM) enriching it with heavy elements, together with their use as standard candles for cosmological distance determination (single-degenerate type Ia supernovae), supernovae (SNe) are extremely interesting phenomena. As interesting are their remnants, which are precious laboratories for collisionless shock physics, particle acceleration and magnetic-field amplification. By studying a large sample of supernova remnants (SNRs) in a given galaxy, we can also reveal global properties of SNRs and SNe, their interactions and parameters of the ISM - abundances, temperatures, density. Search for extragalactic SNRs has an advantage of avoiding heavy Galactic absorption and also dealing with objects with known distances. Galactic SNR sample suffers hardly due to large distance uncertainties.

Optical extragalactic searches for SNRs are mainly done by using the emission line ratio criterion [S II]/H$\alpha > 0.4$ (Mathewson and Clarke 1973, D'Odorico et al. 1980, Fesen et al. 1984, Matonick and Fesen 1997, Blair and Long 1997). This criterion is valid for shock-heated plasmas - sulfur is found in a wide variety of ionization states in the extended recombination zone behind a radiative shock, while

*Based on data collected with 2-m RCC telescope at Rozhen National Astronomical Observatory

in photoionized H II regions it is predominantly in the S^{++} state. So far, more than 1200 optical SNRs in 25 nearby galaxies up to 10 Mpc have been detected (Vučetić et al. 2015 and references therein). Also, optical observations increased the number of the known Galactic SNRs (Stupar et al. 2008, Sabin et al. 2013), which are predominantly discovered in radio-wavelengths. On the other hand, majority of the extragalactic SNRs have been detected in optical wavelengths, as shown in Venn diagrams that summarize the number of SNRs exhibiting emission in different domains in Bozzetto et al. (2017). Nevertheless, only a small number of galaxies have been thoroughly surveyed for SNRs in more than one frequency range and, therefore, it is hard to claim the real status of SNRs in those galaxies. Only Magellanic Clouds, thanks to their vicinity, have majority of SNRs detected simultaneously in the optical, X-ray and radio-domain (Bozzetto et al. 2017). That is why the multiwavelength detection of SNRs in other galaxies is essential for confirmation of SNRs' true nature.

In this paper we present optical photometric search for SNRs in the NGC 2366 galaxy. NGC 2366 is a Magellanic barred irregular galaxy of class IB(s)m (de Vaucouleurs et al. 1991). It is also designated as a blue compact dwarf galaxy (BCDG), which are the least chemically evolved gas-rich star-forming galaxies known in the local Universe (Yin et al. 2011). BCDGs are undergoing intense bursts of star formation, giving birth to thousands of O stars in a very compact starburst region (see e. g. Méndez et al. 1999 for the case of He 10-12 galaxy). NGC 2366 is also known as cometary BCDG, which are characterized by a high surface brightness star-forming region (the comet's head) at one end of an elongated low surface brightness stellar body (the comet's tail). The chain of H II regions extending over galaxy's body is suggestive of self propagating star formation which stopped at the edge of the galaxy. Finally, Micheva et al. (2017) have found that NGC 2366 is an excellent analog of the so called Green Pea galaxies, which are characterized by extremely high ionization parameters.

Table 1. Properties of the NGC 2366 galaxy, taken from NED[1].

Right ascension (J2000)	07h28m54.66s
Declination (J2000)	+69°12′68.″8
Redshift	0.00027
Velocity	80 km s^{-1}
Distance[2]	3.44 Mpc
Angular size	$9.0' \times 3.5'$
Magnitude	10.4 mag
Gal. extinction[3]	0.132 mag (B)

[1] `http://ned.ipac.caltech.edu/`

[2] Tolstoy et al. (1995)

[3] Schlafly and Finkbeiner (2011)

Being a place of intense star formation, this nearby galaxy is a good candidate for SNR searches. So far, this galaxy has been surveyed for radio-SNRs. Using the Very Large Array (VLA), Chomiuk and Wilcots (2009) produced maps at 20, 6, and 3.6 cm with synthesized beams of 3.″7×3.″7 ($\sim 60 \times 60$ pc), and sensitivity of 20 μJy/beam, intended to identify SNRs. Chomiuk and Wilcots (2009) considered discrete radio sources with the non-thermal spectral index $\alpha \leq -0.2$ (defined as $S_\nu \propto \nu^\alpha$), which have the corresponding Hα emission, as SNRs. Non-thermal radio-sources without optical counterparts they classified as probable distant background radio galaxies whose redshifted optical emission, they thought, would fall outside the narrowband Hα filter. We underline here that there are numerous examples of well known and bright radio SNRs with no detected optical emission, such as HFPK334 in Small Magelanic Cloud (Crawford et al. 2014), SNR J0528-6714 in Large Magellanic Cloud (Crawford et al. 2010) or like Vela Jr. (Maxted at al. 2018). Using criteria mentioned above, Chomiuk and Wilcots (2009) suggested five sources – N2366-07, N2366-12, N2366-15, N2366-16 and N2366-18 as SNRs in the NGC 2366 galaxy.

In the next Section, we present our observations of the NGC 2366 galaxy intended to confirm radio SNRs and possibly detect new optical SNR candidates. Furthermore, we used the archival *XMM-Newton* observations of this galaxy to search for possible X-ray counterparts of the SNR candidates. We will discuss and comment individual sources of specific interest in Section 3, and summarize our results in Section 4.

2. OPTICAL OBSERVATIONS

The observations were carried out during multiple observational runs (February 2015, November 2016, March 2017) with the 2-m Ritchey-Chrétien-Coudé (RCC) telescope at the National Astronomical Observatory (NAO) Rozhen, Bulgaria ($\varphi = 41°41'35''$, $\lambda = 24°44'30''$, $h = 1759$ m). The telescope was equipped with VersArray: 1300B CCD camera with 1340×1300 px array, with plate scale of 0.″258/px, giving the field of view $5'45'' \times 5'35''$.

We observed two fields of view (FOV) in order to cover the full extent NGC 2366 galaxy. Centers of the fields of view were: FOV1: R.A.(J2000) = 07:28:34, Decl.(J2000) = +69:10:35; FOV2: R.A.(J2000) = 07:28:58, Decl.(J2000) = +69:14:26.

Additionally, we obtained B, V and R images of the NGC 2366 galaxy on March 29, 2017, from Astronomical station Vidojevica (ASV). Observations were carried out with the 1.4-m Milanković telescope. We took sets of three 5 min exposures through each filter, with seeing 1.″7 – 2.″0. A composite image obtained at ASV, with marked positions of FOV1 and FOV2 taken from NAO Rozhen, is given in Fig. 1. The size of the FOV of the Milanković telescope, with Apogee U42 CCD attached, is $9' \times 9'$.

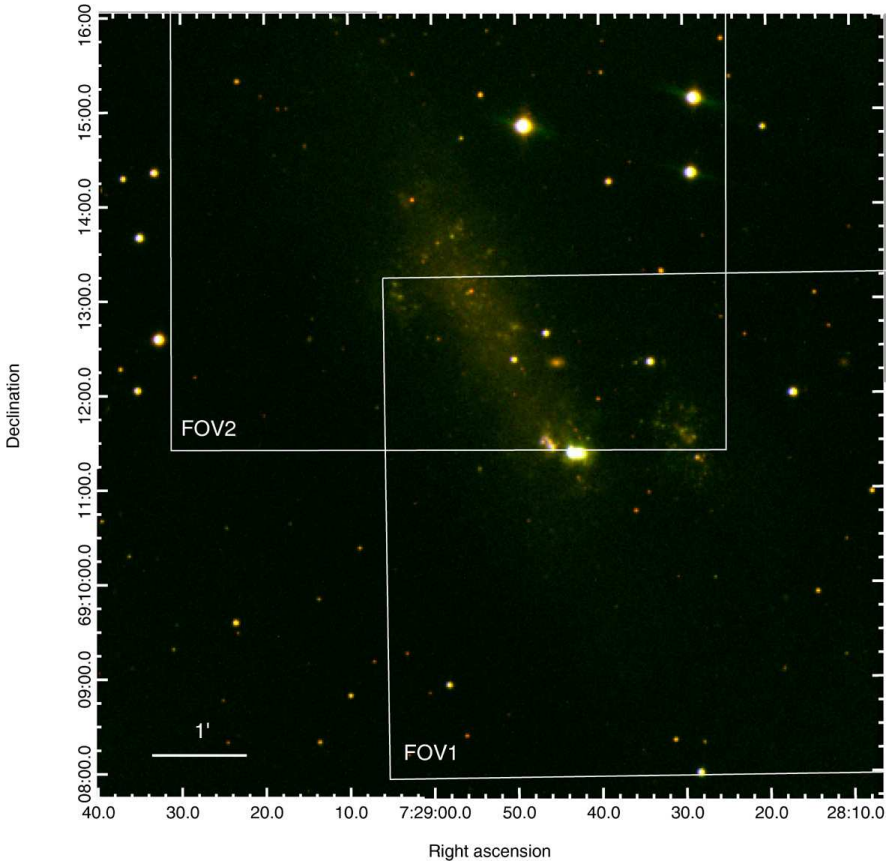

Fig. 1. *Composite image of the NGC 2366 galaxy taken with Milanković telescope. Red color is for the R filter, green is for the V filter and blue is for the B filter. Size of the FOV is* $9' \times 9'$*. FOV1 and FOV2 were observed from NAO Rozhen.*

The observations from NAO Rozhen were performed with the narrowband [S II], Hα and red continuum filters, each wide approximately 30 Å. FOV1 was observed with the total exposure times of 160 min (continuum), 100 min (Hα) and 60 min ([S II] filter), with median seeing of $2\farcs5$ – $3\farcs25$. FOV2 was observed with the total exposure times of 125 min (continuum), 135 min (Hα) and 60 min ([S II] filter), with median seeing of $1\farcs75$ – $2\farcs0$. Images of the standard star Feige 34, as well as sky flat-field images, were also taken.

Data reduction was done by using standard procedures in IRAF[1] and IRIS[2]. Images through each filter were firstly combined using the sigma-clipping method, then sky-subtracted, and finally flux calibrated using the observations of the standard star Feige 34 and its fluxes from Oke (1990). Afterwards, the continuum contribution was removed from the Hα and [S II] images, scaling each image to have the same flux for 20 foreground stars in the field, prior to the continuum subtraction. Continuum-subtracted Hα images were corrected for the filter transmission and contamination by the [N II] lines at λ6548 Å, λ6583 Å, using the median [N II]λ6548/Hα ratio obtained from spectra of 61 H II regions detected in NGC 2366 by Roy et al. (1996). Since there were no previous optical SNR detections, we used the same [N II]λ6548/Hα ratio for our SNR candidates. Also, emission from the [S II] lines at λ6717 Å, λ6731 Å, was corrected for filter transmission, as suggested in Vučetić et al. (2013).

2.1. Hα detected objects

In Figs. 2 and 3 we present the continuum subtracted Hα images of FOV1 and FOV2, and in Fig. 4 we present the continuum subtracted [S II] image of FOV2, which shows all sources with the [S II] emission. Displayed images are zoomed-in in order to show only the regions where the emission nebulae were detected. We detected 67 Hα sources, most

[1]IRAF is distributed by the National Optical Astronomy Observatory, which is operated by the Association of Universities for Research in Astronomy, Inc., under cooperative agreement with the National Science Foundation.

[2]Available from `http://www.astrosurf.com/buil/`

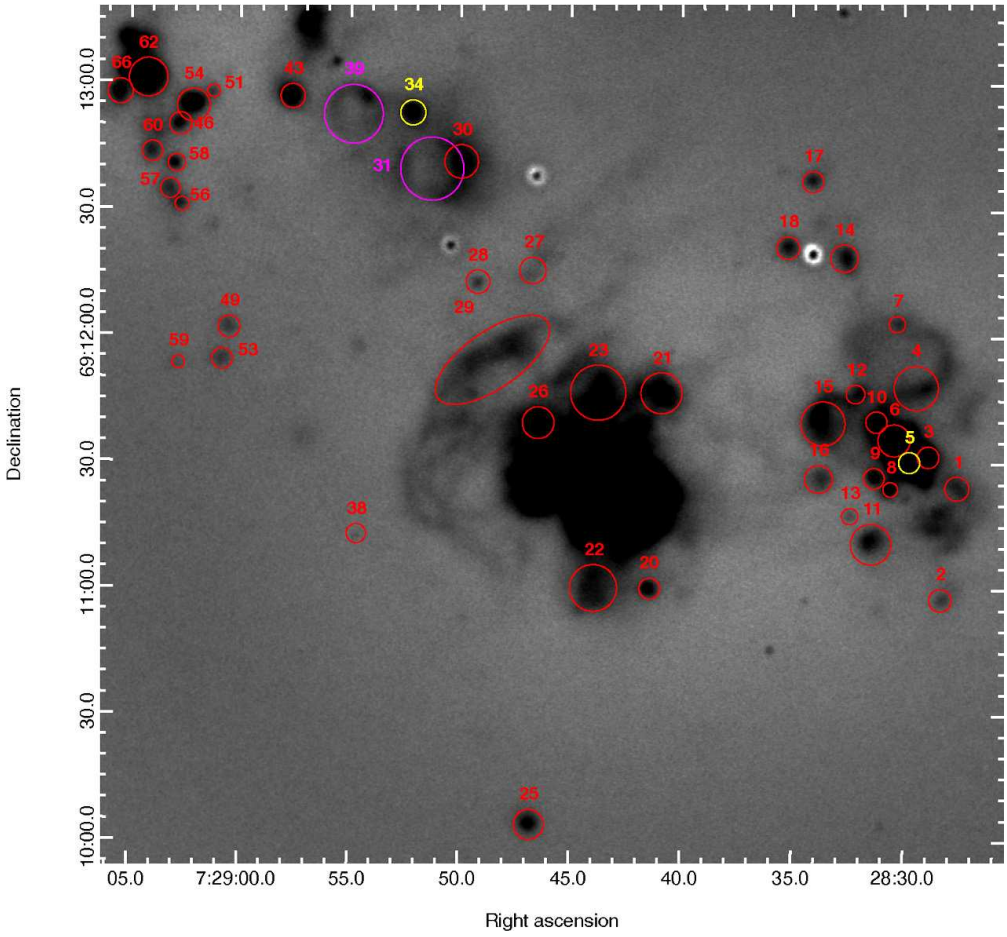

Fig. 2. *Hα-continuum subtracted image of NGC 2366 - FOV1, taken from NAO Rozhen. Properties of marked objects are given in Table 2. Objects marked with yellow color are the SNR candidates, while objects marked with magenta color are superbubbles. Non-marked objects are stars and the center of the galaxy where the continuum was not subtracted well.*

probably the H II regions, filaments and superbubbles.

We suggest two sources (Vu19 5 and Vu19 34) as optical SNR candidates according to their enhanced [S II] emission, and detected counterparts in the radio and X-ray domain (see Section 3). Coordinates, diameters, Hα fluxes and [S II]/Hα ratios for detected objects are given in Table 2. We emphasize here that [S II]/Hα ratios for SNR candidates are probably underestimated, since Hα fluxes of SNR candidates given in Table 2 are corrected for the [N II] contamination in the same way as H II regions, while it is expected that shock-heated objects have enhanced [N II] lines. This would lead to overestimation of the Hα flux for SNRs and therefore to underestimation of the [S II]/Hα ratio. We add that the given diameters in Table 2 are overestimated since the observations were made under seeing conditions of $3\farcs25$ for FOV1 and $2\farcs0$ for FOV2, which equals to linear size of 55 pc and 35 pc, respectively. Majority of the detected H II regions and filaments were already detected by Hodge and Kennicutt (1983), Roy et al. (1996), and Eymeren et al. (2007), but without previously reported Hα fluxes. We propose two objects as superbubbles (Vu19 31 and Vu19 39) according to their diameters (240 pc and 250 pc) and the present [S II] emission, and one object as a giant supershell (Vu19 67), which has size above 500 pc.

Five of our objects (Vu19 5, 27, 34, 38, 44) were detected in radio wavelengths and were suggested to be SNR candidates based on their radio-spectral index (Chomiuk and Wicots 2009). Our observations also suggest objects Vu19 5 and Vu19 34 as SNR candidates, while we discard objects Vu19 27 and Vu19 38 as SNRs (see Section 3 for more details). In the vicinity of Vu19 27, which is really marginally detected in the Hα image, there is a bright continuum source, separated by about 5 arcseconds from Vu19 27, whose appearance is galaxy-like. This continuum source could match the radio source N2366-12 from Chomiuk and Wicots (2009) and, since it does not have the Hα counterpart, it could not be

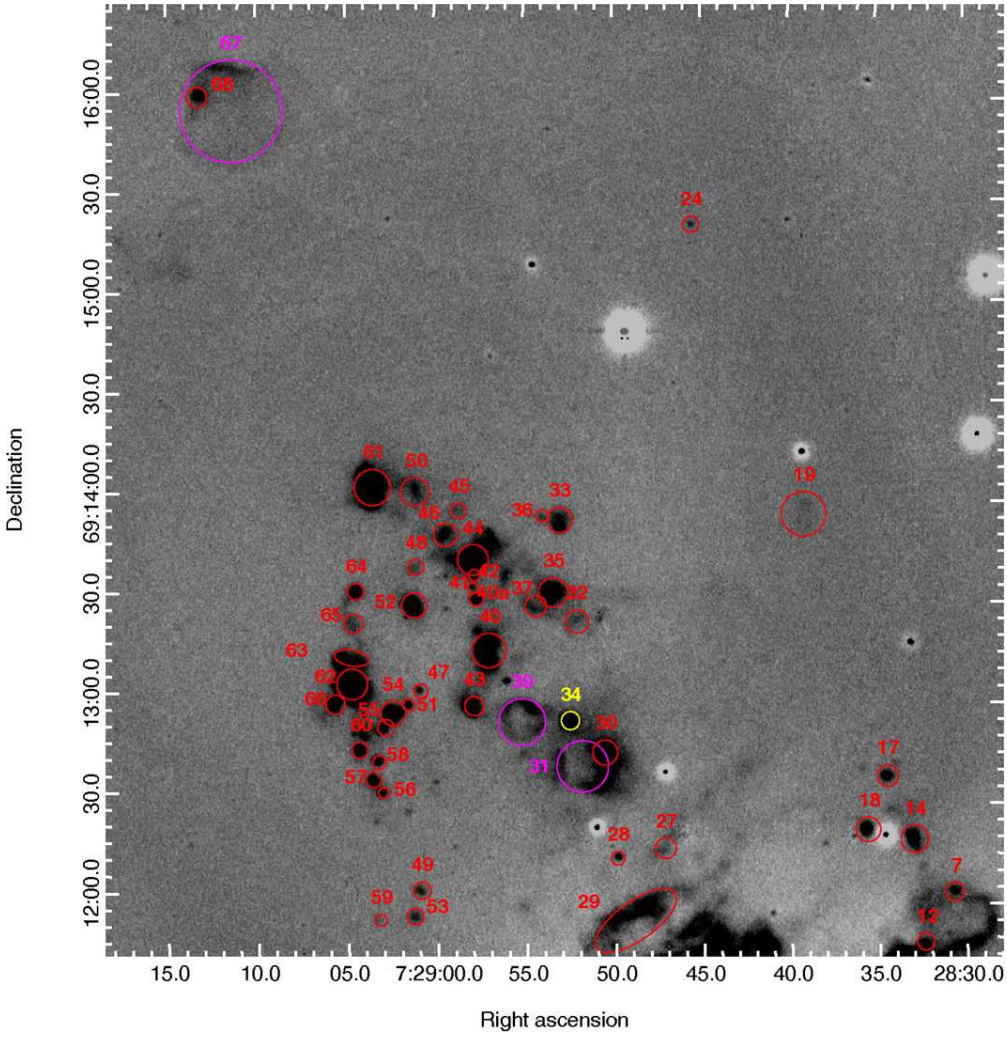

Fig. 3. *Hα-continuum subtracted image of NGC 2366 - FOV2, taken from NAO Rozhen. Properties of marked objects are given in Table 2. The object marked with yellow color is a SNR candidate, while objects marked with magenta color are superbubbles. Non-marked objects are stars, where continuum was not subtracted well.*

an SNR. This object has also been catalogued as a galaxy in the 2MASS catalogue as 2MASX J07284539+6912186 and a background galaxy N2366BG7 in Drissen et al. (2000). The object Vu19 38 appears only in the continuum image and is most probably a background galaxy (see Section 3.3 for more details).

3. ARCHIVAL XMM-NEWTON OBSERVATIONS OF NGC 2366

As previously mentioned, BCDGs are undergoing intense bursts of star formation. Because of the presence of many massive short-lived stars, BCDGs are expected to emit in X-rays. This X-ray emission can originate from compact sources such as high-mass X-ray binaries (HMXBs) and/or hot O and Wolf-Rayet stars, or from diffuse sources like hot plasma associated with SNRs or superbubbles (Sano et al. 2017, Kavanagh et al. 2019). NGC 2366 was observed by the *XMM-Newton* Observatory with all EPIC cameras using the medium filter in full field mode (ObsId 0141150201, PI: T. X. Thuan). Thuan et al. (2014) suggested that NGC 2366 contains two faint X-ray point sources and two faint extended sources. According to them, one point source (XMMU J072858.2+691134) is likely to be a background AGN, while the other (XMMU J072855.4+691305) appears to be coincident with a very luminous star associated with NGC 2366. On the other hand, the X-ray luminosity of this object would be comparable to Galactic accreting or colli-

ding-wind HMXBs, suggesting the foreground star scenario. Therefore, identification of the object XMMU J072855.4+691305, whose optical counterpart is visible in Fig. 3 as point-source above the object Vu19 39, is very intriguing and still not unique. The two faint extended sources are associated with massive H II complexes. In Fig. 5 we present an adaptively-smoothed exposure-corrected combined *XMM-Newton* EPIC image of the NGC 2366 main parts (scaled with minmax/log and 25 smoothing counts). The image depicts emission detected over the energy range from 0.4 keV to 7.0 keV. Some of the optically detected sources are represented by white circles. The X-ray data were analyzed by using standard tools of the HEASOFT Software Package and the Science Analysis Software (SAS) software package (Version 17.0.0). The SAS tools `epchain` and `emchain` were used to apply standard processing tools to the EPIC datasets while the tools `mos-filter` and `pn-filter` were used to filter data for the background flaring activity. The effective exposure times of the MOS1/2 and PN cameras were 39 and 29 ks, respectively. The *XMM-Newton* astrometric accuracy is ≈2 – 4 arcsec (Watson et al. 2009).

3.1. SNR candidate Vu19 5

We have found that our objects Vu19 5 and Vu19 6 are in fact coincident with faint soft X-ray source XMMU J072830.4+691132 (see Fig. 5). Actually, in the analysis of X-ray sources spatially coincident with NGC 2366, Thuan et al. (2014) only noted that the extent of this X-ray source aligns well with a dense stellar cluster and a massive H II complex according to the position alignment with the Hubble Space Telescope (*HST*) F814W image (see Fig. 4 in Thuan et al. 2014). We used the *HST* Wide-Field Planetary Camera 2 (WFPC2) image through the F656N filter (Proposal ID 6096, PI Drissen L.) to resolve this complex starforming region (also known as NGC2363), where we label our objects 3, 5, 6, 8, 9, and 10. On the *HST* WFPC2 image we overlaid [S II] contours (Fig. 6). It looks like the position of object Vu19 5 covers at least two Hα objects resolved with *HST*. One on the border with the object Vu19 3, is more compact and the other on the border with the object Vu19 6 exhibits partial-shell structure with the diameter of 62 pc.

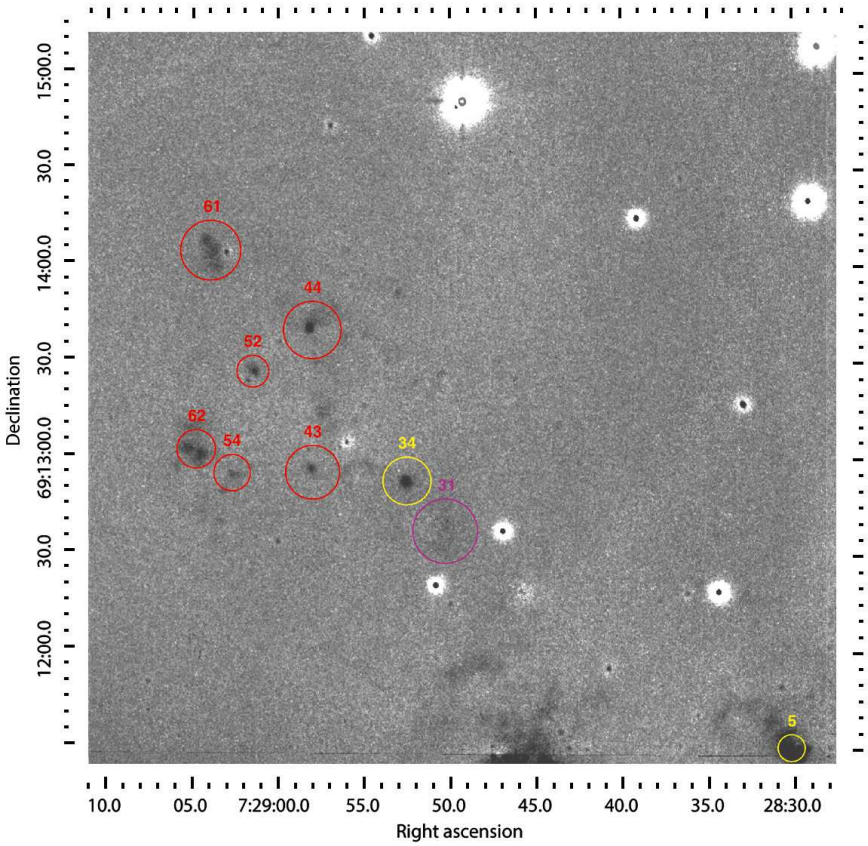

Fig. 4. *[S II]-continuum subtracted image of NGC 2366 - FOV2, taken from NAO Rozhen. Properties of marked objects are given in Table 2.*

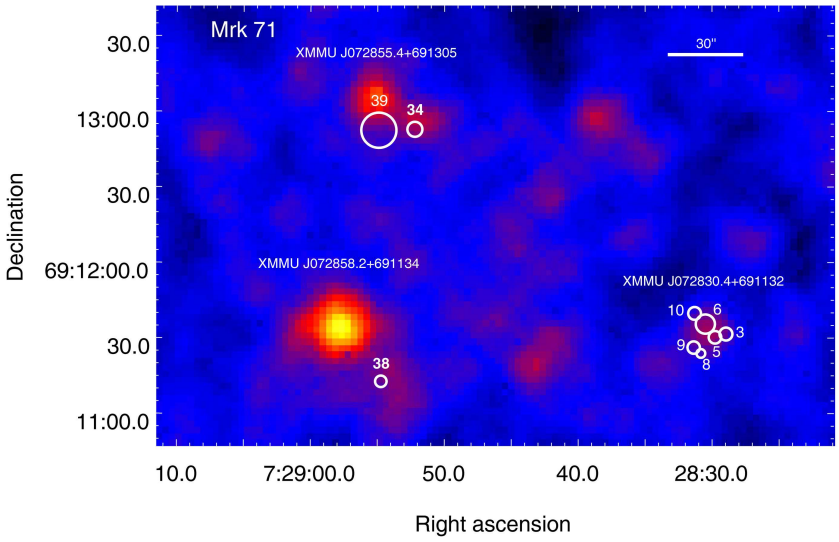

Fig. 5. *Adaptively-smoothed exposure-corrected combined XMM-Newton EPIC image of the NGC 2366 main parts. The image depicts emission detected over the 0.4 keV to 7.0 keV energy range. Some of the optically detected sources are represented by white circles.*

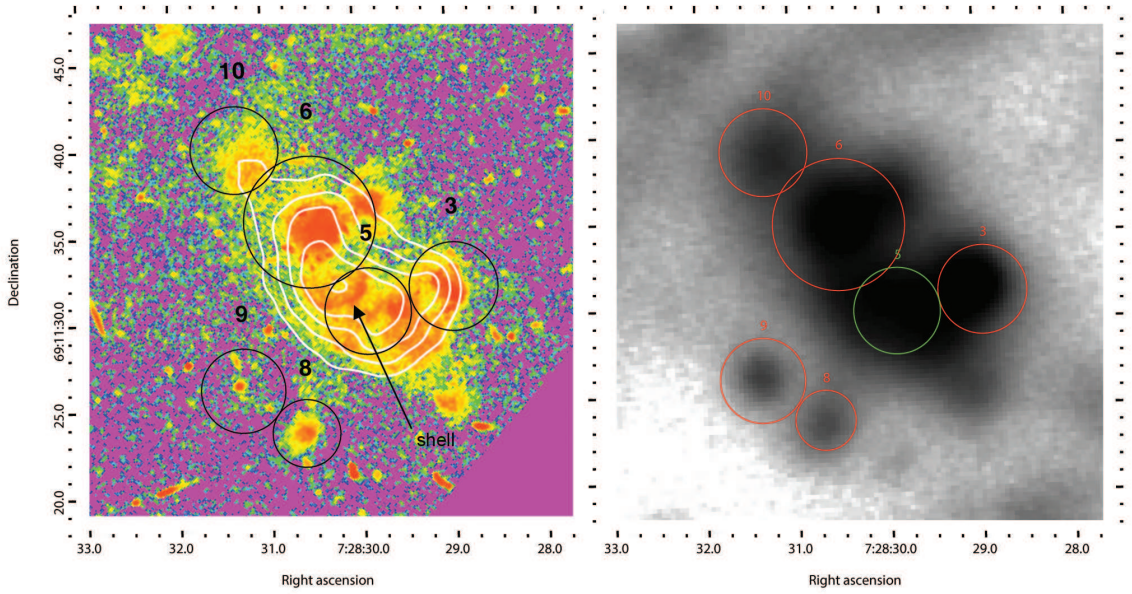

Fig. 6. *Left: HST WFPC2 F658N image with overlaid [S II] contours, centered on the starforming region near the object Vu19 5. The maximum of [S II]emission aligns with the partial Hα shell resolved with HST. Right: the same part of our Hα image. Seeing was 3.″25. The diameter of the SNR candidate Vu19 5 is 5.″0=85 pc.*

This shell-like structure is coincident with the maximum of the [S II] emission and we propose that this object could be the optical SNR candidate Vu 19 5, which has an X-ray counterpart. Although the measured [S II]/Hα ratio of this object is 0.21, we emphasize that the given [S II]/Hα ratios are likely underestimated for SNRs (as explained in Section 2.1), and that the unresolved area of the SNR candidate Vu19 5 probably covers emission of an H II region as well. Unfortunately, the current *XMM-Newton* data are not sufficient to definitely characterize the spectral nature of this X-ray emission. In addition, this source is also included in the *XMM-Newton* Serendipitous Source Catalog 3XMM DR8 Version (3XMM J072830.1+691132) with rather low detection maximum likelihood of 7.45, and hardness

Table 2. Properties of Hα emitting regions in the NGC 2366 galaxy.

Object ID	Right Ascension α_{J2000}	Decl. δ_{J2000}	Hα flux* [erg s^{-1} cm^{-2}] $\times 10^{-15}$	Diameter** [pc]	[S II]/Hα ratio	Comment
Vu19 1	07:28:27.7	+69:11:24	31.70	110		H II region
Vu19 2	07:28:28.4	+69:10:58	1.74	90		H II region
Vu19 3	07:28:29.0	+69:11:32	14.61	80		H II region
Vu19 4	07:28:29.5	+69:11:48	0.00	180		filament
Vu19 5[a]	07:28:30.7	+69:11:33	11.31	62†	0.21	SNR candidate
Vu19 6	07:28:30.5	+69:11:36	16.70	130		H II region
Vu19 7	07:28:30.3	+69:12:03	1.04	60		part of a filament
Vu19 8	07:28:30.8	+69:11:24	2.58	60		H II region
Vu19 9	07:28:31.4	+69:11:27	2.73	80		H II region
Vu19 10	07:28:31.3	+69:11:40	5.04	80		H II region
Vu19 11	07:28:31.5	+69:11:11	5.91	160		H II region
Vu19 12	07:28:32.2	+69:11:47	1.49	70		H II region
Vu19 13	07:28:32.6	+69:11:18	0.51	50		H II region
Vu19 14	07:28:32.8	+69:12:19	4.03	70		H II region
Vu19 15	07:28:33.7	+69:11:40	5.41	180		H II reg. surrounded by filaments
Vu19 16	07:28:33.9	+69:11:26	2.45	110		giant H II region
Vu19 17	07:28:34.2	+69:12:37	2.32	110		giant H II region
Vu19 18	07:28:35.4	+69:12:22	3.59	70		H II region
Vu19 19	07:28:38.9	+69:13:55	/	220		very faint H II region
Vu19 20	07:28:41.6	+69:11:00	3.70	80		H II region
Vu19 21	07:28:40.9	+69:11:46	12.72	160		giant H II region
Vu19 22	07:28:44.0	+69:11:00	11.05	190		diffuse
Vu19 23	07:28:43.8	+69:11:47	21.32	220		giant H II region
Vu19 24	07:28:45.3	+69:15:22	0.50	80		H II region
Vu19 25	07:28:46.9	+69:10:05	4.93	120		giant H II region
Vu19 26	07:28:46.5	+69:11:40	3.78	130		giant H II region
Vu19 27[b]	07:28:46.8	+69:12:16	/	/		not SNR; see Section 2.1
Vu19 28	07:28:49.2	+69:12:13	0.61	90		H II region
Vu19 29	07:28:48.6	+69:11:54	0.00	540 × 230		filament
Vu19 30	07:28:50.2	+69:11:39	8.06	230		giant H II region
Vu19 31	07:28:51.3	+69:12:40	5.52	250	0.11	superbubble
Vu19 32	07:28:51.8	+69:13:23	1.19	120		giant diffuse
Vu19 33	07:28:52.7	+69:13:53	5.54	130		giant H II region
Vu19 34[c]	07:28:52.3	+69:12:53	5.47	80	0.38	SNR candidate
Vu19 35	07:28:53.1	+69:13:31	11.16	150		giant H II region
Vu19 36	07:28:53.7	+69:13:54	0.78	60		H II region
Vu19 37	07:28:54.1	+69:13:27	2.02	110		diffuse
Vu19 38[d]	07:28:54.7	+69:11:12	0.15	80		not SNR; see Section 3.3
Vu19 39	07:28:54.9	+69:12:52	5.52	240	0.09	superbubble
Vu19 40	07:28:56.7	+69:13:13	5.31	170		H II region
Vu19 40a	07:28:57.4	+69:13:29	2.48	70		H II region
Vu19 41	07:28:57.5	+69:13:33	0.42	50		H II region
Vu19 42	07:28:57.5	+69:13:36	1.06	60		H II region
Vu19 43	07:28:57.7	+69:12:57	13.42	100	0.06	giant H II region

*Reddening corrected (Schlafly and Finkbeiner 2011).

**One arcsec corresponds to 17 pc for the assumed distance to NGC 2366 of 3.44 Mpc.

†This diameter is given according to the size of the corresponding shell detected with *HST* (see Section 3.1).

Chomiuk and Wilcots (2009) radio-SNR IDs: [a] N2366-07; [b] N2366-12; [c] N2366-15; [d] N2366-16.

Table 2. Continued.

Object ID	Right ascension α_{J2000}	Decl. δ_{J2000}	Hα flux* [erg s^{-1} cm^{-2}] $\times 10^{-15}$	Diameter** [pc]	[S II]/Hα ratio	Comment
Vu19 44[e,f]	07:28:57.7	+69:13:41	30.40	160	0.06	giant H II region
Vu19 45	07:28:58.4	+69:13:55	0.78	80		H II region
Vu19 46	07:28:59.1	+69:13:27	2.25	40		H II region
Vu19 47	07:29:00.6	+69:13:02	0.78	70		H II region
Vu19 48	07:29:00.8	+69:13:38	0.85	80		diffuse
Vu19 49	07:29:00.5	+69:12:02	1.52	90		H II region
Vu19 50	07:29:00.8	+69:14:01	1.62	140		diffuse
Vu19 51	07:29:01.3	+69:12:58	1.50	50		H II region
Vu19 52	07:29:01.0	+69:13:30	14.32	130		H II region
Vu19 53	07:29:00.8	+69:11:54	1.46	80		H II region
Vu19 54	07:29:02.1	+69:12:55	10.57	130	0.05	H II region
Vu19 55	07:29:02.8	+69:12:51	2.37	80		H II region
Vu19 56	07:29:02.7	+69:12:31	1.82	50		H II region
Vu19 57	07:29:03.2	+69:12:35	1.71	80		H II region
Vu19 58	07:29:03.0	+69:12:41	1.99	70		H II region
Vu19 58	07:29:02.7	+69:11:54	0.52	50		H II region
Vu19 60	07:29:03.9	+69:12:44	1.89	80		H II region
Vu19 61	07:29:03.5	+69:14:02	36.83	180	0.10	diffuse
Vu19 62	07:29:04.3	+69:13:04	55.61	150	0.06	H II region
Vu19 63	07:29:04.5	+69:13:11	9.59	170×80		H II region
Vu19 64	07:29:04.2	+69:13:31	3.67	80		H II region
Vu19 65	07:29:04.3	+69:13:22	1.50	90		H II region
Vu19 66	07:29:05.4	+69:12:57	4.22	90		H II region
Vu19 67	07:29:11.4	+69:15:55	15.66	520		giant superbubble
Vu19 68	07:29:13.1	+69:15:59	2.61	100		H II region

*Reddening corrected (Schlafly and Finkbeiner 2011).

**One arcsec corresponds to 17 pc for an assumed distance to NGC 2366 of 3.44 Mpc.

Chomiuk and Wilcots (2009) radio-SNR IDs: [e] N2366-18.

[f] Also designated as N2366BG14 background galaxy in the field of NGC 2366 (Drissen et al. 2000), and compact star cluster (Billett et al. 2002).

ratios $HR_1 > 0$ and $HR_2 < 0$ that are in a good accordance with the conclusions stated in Sasaki et al. (2018) for the known SNRs in the northern disc of the M31 galaxy (see also Sturm et al. 2013 for definition of HRs). At the position of the border of regions 5 and 6, coincident with the shell, Chomiuk and Wilcots (2009) detected the object N2366-07 characterized as SNR. This object has the radio spectral index $\alpha = -0.53 \pm 0.04$, size of 73×63 pc, and flux density 0.20 mJy at 20 cm.

3.2. SNR candidate Vu19 34

Thuan et al. (2014) also mentioned a faint potential X-ray point source, slightly blended with XMMU J072855.4+691305. This could be an X-ray counterpart of the possible optical SNR, labeled as Vu19 34 in our analysis (see Fig. 5), also detected at radio frequencies (Chomiuk and Wilcots 2009). Radio source N2366-15, coincident with the SNR candidate Vu19 34, has the spectral index $\alpha = -0.37 \pm 0.07$, size of 70×63 pc, and flux density 0.19 mJy at 20 cm. The optical diameter of object Vu19 34 is 80 pc, which suggests that this SNR candidate is in a late radiative phase. With the present X-ray data it is not possible to thoroughly examine the nature of this X-source. However, we note that the radio, optical and X-ray detection suggests an SNR origin of the source (see Filipović et al. 1998, Long 2017, Bozzetto et al. 2017).

3.3. Object Vu19 38

Near the bright X-ray source XMMU J072858.2+691134, likely a background galaxy hosting an AGN, a very faint X-ray emission is detected. Due to the angular proximity, we cautiously note that this could be an X-ray counterpart to the object Vu19 38 (see Fig. 5). This object is most probably a background galaxy, or a pair of interacting galaxies

labeled as N2366BG13 and N2366BG14 in Drissen et al. (2000), or a compact star cluster (marked as cluster 2 in Billet et al. 2000). Of course, such a conclusion can not be strongly verified with this particular X-ray observation. Chomiuk and Wilcots (2009) detected the radio object N2366-16 at the position of Vu19 38, and they suggested that it is an SNR. According to its optical appearance, being bright in the continuum filter (at λ6417 Å), and its non-detection in the Hα filter, we definitely discard it as an SNR candidate.

4. SUMMARY

In this paper, we presented optical observations of the nearby irregular galaxy NGC 2366. This was the first time that this galaxy was observed through the [S II] filter, i.e. with the intention to detect optical SNR candidates. Besides 64 probable H II regions and filaments, and three superbubbles, we suggested two objects as SNR candidates - Vu19 5 and Vu19 34. We underline that our observations were done with a rather poor seeing condition (up to $3\farcs25$=55 pc for FOV1 and $2\farcs0$=35 pc for FOV2) which probably led to non-detection of potential SNRs with smaller than seeing-limited diameter, and SNRs in crowded starforming regions. The archival *HST* WFPC2 image through an F656N filter showed a shell-like structure at the position of the SNR candidate Vu19 5. Also, archival *XMM-Newton* observations suggest possible faint X-ray counterparts to two of our optical SNR candidates, which have also been detected with VLA and previously designated as radio-SNRs by Chomiuk and Wilcots (2009). In addition, according to their optical appearance and former identifications as background galaxies resolved with *HST*, we discard two previous radio SNR candidates in this galaxy. This suggests that, so far, the NGC 2366 galaxy hosts three SNR candidates, two visible in optical, X-ray and radio-domain, and one radio SNR candidate.

Acknowledgements – This research has been supported by the Ministry of Education, Science and Technological Development of the Republic of Serbia through the project No. 176005 "Emission nebulae: structure and evolution" and it is a part of the joint project of Serbian Academy of Sciences and Arts and Bulgarian Academy of Sciences "Optical search for supernova remnants and H II regions in nearby galaxies (NGC 2366 and NGC 5585)". Authors thank Dragana Ćiprijanović for help with image editing. Authors gratefully acknowledge observing grant support from the Institute of Astronomy and the Rozhen National Astronomical Observatory, Bulgarian Academy of Sciences. This research has made use of data obtained from the 3XMM XMM-Newton serendipitous source catalogue compiled by the 10 institutes of the *XMM-Newton* Survey Science Centre selected by ESA.

REFERENCES

Billett, O. H. and Hunter, D. A.: 2002, *Astron. J.*, **123**, 1454.
Blair, W. P. and Long, K. S.: 1997, *Astrophys. J. Suppl. Series*, **108**, 261.
Bozzetto, L. M., Filipović, M. D., Vukotić, B., Pavlović, M. Z., Urošević, D., Kavanagh, P. J., Arbutina, B., Maggi, P. et al.: 2017, *Astrophys. J. Suppl. Series*, **230**, 2.
Chomiuk, L. and Wilcots, E. M.: 2009, *Astron. J.*, **137**, 3869.
Crawford, E. J., Filipović, M. D., Haberl, F., Pietsch, W., Payne, J. L. and de Horta, A. Y.: 2010, *Astron. Astrophys.*, **518**, 35.
Crawford, E. J., Filipović, M. D., McEntaffer, R. L., Brantseg, T., Heitritter, K., Roper, Q., Haberl, F. and Urošević, D.: 2014, *Astron. J.*, **148**, 99.
de Vaucouleurs, G., de Vaucouleurs, A., Corwin, H. G., Jr., et al.: 1991, Third Reference Catalogue of Bright Galaxies, Springer, New York.
Drissen, L., Jean-ReneRoy, J.-R., Robert, C. and Devost, D.: 2000, *Astron. J.*, **119**, 688.
D'Odorico, S., Dopita,M. A. and Benvenuti, P.: 1980, *Astron. Astrophys. Suppl. Series*, **40**, 67.
Fesen, R. A., Blair,W. P. and Kirshner, R. P.: 1985, *Astrophys. J.*, **292**, 29.
Filipović, M. D., Haynes, R. F., White, G. L. and Jones, P. A.: 1998, *Astron. Astrophys. Suppl. Series*, **130**, 421.
Hodge, P. W. and Kennicutt, R. C. Jr.: 1983, *Astron. J.*, **88**, 296.
Kavanagh, P. J., Vink, J., Sasaki, M., Chu, Y.-H., Filipović, M. D., Ohm, S., Haberl, F., Manojlović, P. and Maggi, P.: 2019, *Astron. Astrophys.*, **621**, 138.
Long, K. S.: 2017, in "Handbook of Supernovae", eds. A. W. Alsabti and P. Murdin, Springer International Publishing.
Mathewson, D. S. and Clarke, J. N.: 1973, *Astrophys. J.*, **178**, 105.
Matonick, D. M. and Fesen, R. A.: 1997, *Astrophys. J. Suppl. Series*, **112**, 49.
Maxted, N. I., Filipović, M. D., Sano, H., Allen, G. E., Pannuti, T. G., Rowell, G. P., Grech, A., Roper, Q. et al.: 2018, *Astrophys. J.*, **866**, 76.
Méndez, D. I., Esteban, C., Filipović, M. D., Ehle, M., Haberl, F., Pietsch, W. and Haynes, R. F.: 1999, *Astron. Astrophys.*, **349**, 801.
Micheva, G., Oey, M. S., Jaskot, A. E. and James, B. L.: 2017, *Astrophys. J.*, **845**, 165.
Oke, J. B.: 1990, *Astron. J.*, **99**, 1621.
Roy, J.-R, Belley, J., Dutil, Y. and Martin, P.: 1996, *Astrophys. J.*, **460**, 284.
Sabin, L., Parker, Q. A., Contreras, M. E., Olgun, L., Frew, D. J., Stupar, M., Vzquez, R., Wright, N. J. et al.: 2013, *Mon. Not. R. Astron. Soc.*, **431**, 279.
Sano, H. et al.: 2017, *Astrophys. J.*, **843**, 61.
Sasaki, M., Haberl, F., Henze, M., Saeedi, S., Williams, B. F., Plucinsky, P. P., Hatzidimitriou, D., Karampelas, A. et al.: 2018, *Astron. Astrophys.*, **620**, 28.

Schlafly, E. F. and Finkbeiner, D. P.: 2011, *Astrophys. J.*, **737**, 103.
Stupar, M., Parker, Q. A. and Filipović, M. D.: 2008, *Mon. Not. R. Astron. Soc.*, **390**, 1037.
Sturm, R., Haberl, F., Pietsch, W., Ballet, J., Hatzidimitriou, D., Buckley, D. A. H., Coe, M., Ehle, M. et al.: 2013, *Astron. Astrophys.*, **558**, 3.
Thuan, T. X., Bauer, F. E. and Izotov, Y. I.: 2014, *Mon. Not. R. Astron. Soc.*, **441**, 1841.
Tolstoy, E., Saha, A., Hoessel, J. G. and McQuade, K.: 1995, *Astron. J.*, **110**, 164.
van Eymeren, J., Bomans, D. J., Weis, K. and Dettmar, R.-J.: 2007, *Astron. Astrophys.*, **474**, 67.
Vučetić, M. M., Arbutina, B., Urošević, D., Dobardžić, A., Pavlović, M. Z., Pannuti, T. G. and Petrov, N.: 2013, *Serb. Astron. J.*, **187**, 11.
Vučetić, M. M., Arbutina, B. and Urošević, D.: 2015, *Mon. Not. R. Astron. Soc.*, **446**, 943.
Watson, M. G. et al.: 2009, *Astron. Astrophys.*, **493**, 339.
Yin, J., Matteucci, F. and Vladilo, G.: 2011, *Astron. Astrophys.*, **531**, 136.

ОПТИЧКА ПОСМАТРАЊА БЛИСКЕ ГАЛАКСИЈЕ NGC 2366 КРОЗ УСКОПОЈАСНЕ ФИЛТЕРЕ [SII] И Hα. СТАТУС ОСТАТАКА СУПЕРНОВИХ

M. M. Vučetić[1], D. Onić[1], N. Petrov[2], A. Ćiprijanović[1] and M. Z. Pavlović[1]

[1] *Department of Astronomy, Faculty of Mathematics, University of Belgrade, Studentski trg 16, 11000 Belgrade, Serbia*

E–mail: *mandjelic@math.rs, donic@math.rs, aleksandra@math.rs, marko@math.rs*

[2] *Institute of Astronomy and National Astronomical Observatory, Bulgarian Academy of Sciences, 72 Tsarigradsko Shosse Blvd, BG-1784 Sofia, Bulgaria*

E–mail: *nip.sob@gmail.com*

УДК 520.822 + 524.7 NGC2366 + 524.354
Оригинални научни рад

У раду је презентована детекција 64 HII региона, три супермехура и два оптичка кандидата за остатаке супернових (ОСН) у оближњој неправилној галаксији NGC 2366. Детекција је извршена употребом критеријума везаног за однос [S II] и Hα линија, користећи посматрања са двометарског телескопа Националне астрономске опсерваторије Рожен у Бугарској. У раду су дати положаји, дијаметри, као и Hα и [S II] флуксеви детектованих објеката у два посматрана видна поља у галаксији NGC 2366. На основу архивских посматрања рентгенског телескопа XMM-Newton уочена су два извора слабог сјаја која одговарају оптичким кандидатима за ОСН. Такође, на основу оптичких посматрања закључујемо да је претходно предложена класификација два објекта као радио-ОСН вероватно погрешна, те да су то највероватније позадинске галаксије.